

PRACTICAL SECURITY-BOUNDARY-CONSTRAINED DISPATCH MODELS FOR ELECTRICITY MARKETS

Claudia Battistelli¹, Claudio A. Cañizares², Mohammad Chehreghani Bozchalui²,
Victor J. Gutierrez-Martinez³, Claudio R. Fuerte-Esquivel³

¹ Federico II University, Naples, Italy

² University of Waterloo, Waterloo, Canada

³ Universidad Michoacana de San Nicolás de Hidalgo, Morelia, Mexico
ccanizar@uwaterloo.ca

Abstract – This paper concentrates on a robust characterization of system security, in terms of voltage collapse and oscillatory instabilities, in a “typical” multi-period DC-OPF auction and dispatch model. This characterization is based on the representation of the system security limits by means of a Neural Network (NN) approximation of the system security boundary. The proposed model is tested and compared with respect to a typical multi-period Security Constrained DC-OPF (SC-DC-OPF) model using the well-known two-area benchmark system. Results demonstrate that the approach ensures, in general, better locational marginal prices (LMPs) and guarantees that the operating points resulting from the optimization solution process are within the desired feasible and secure region, contrary to the typical multi-period SC-DC-OPF model, which may fail to meet this condition.

Keywords: *Optimal power flow, security constraints, neural networks, electricity markets, power dispatch, locational marginal pricing.*

1 INTRODUCTION

In the context of deregulated electricity markets, power systems operating close to their security limits have significant effect on prices and overall operating costs [1]. On the other hand, stability problems, particularly voltage collapse and oscillatory instabilities, have led to significant concerns on the part of system operators regarding the secure operation of power networks [2]. Therefore, the proper representation of system security in auction and dispatch models typically used by system operators for clearing and dispatching power markets has become quite relevant, since the typical accounting of system security by means of simple power transfer limits on transmission lines could prove to be inadequate [1]. The latter is due the fact that transmission limits do not always represent the actual security levels directly associated with the current market and system conditions, since they are determined off-line based on system operating conditions that do not necessarily correspond to the actual dispatch scenarios, which are mostly driven by market conditions at the time of dispatch, resulting in some cases in insecure operating conditions and/or inappropriate price signals [1], [3].

Several approaches to properly represent system security in OPF models, which are the base for market clearance and dispatch tools, have been proposed. For example, in [4], a stability-constrained OPF model is proposed based on a time-domain numerical representa-

tion of the dynamic equations which are included as constraints in the OPF process. In [5], a somewhat similar time-domain dispatch algorithm is proposed, but considering contingencies. In [6], the authors compare two different approaches to represent voltage security limits within OPF models; one is based on using the MSV of the power flow Jacobian, which is an index to detect proximity to voltage instability, as a security constraint, whereas the other is based on introducing the power flow equations associated with the voltage collapse point as additional constraints. An enhancement to the MSV approach is presented in [7], where oscillatory and voltage instability conditions are represented through a “dynamic” MSV stability index. The stability index used in [6] and [7] is an implicit function of the optimization variables, and hence their derivatives can be only approximated numerically in order to be included in the OPF solution process, leading to convergence problems and an approximation of the actual security limits. An improvement to this approach is presented in [8], where an MSV of an “equivalent” power flow Jacobian and an iterative procedure are proposed to explicitly represent the MSV security constraint in the OPF model. Finally, a differentiable function that can be readily introduced as a security constraint in an OPF model is proposed in [9]; in this case, the stability boundary is approximated by a polynomial obtained from an interpolation procedure and a nonlinear transformation applied to the system state variables.

All of proposed improvements available in the literature for the proper representation of security limits within dispatch and auction models are based on detailed and somewhat complex AC-OPF models. However, in practice, market clearing and dispatch mechanisms are based on DC-OPF multi-period models [3], given their significant computation advantages [10], such as less CPU-intensive computations and linear characteristics, which become more relevant in the multi-period models needed to represent ramp rates limits of generation units. Therefore, the current paper concentrates on the better representation of system security limits in a multi-period DC-OPF auction and dispatch model.

Extensive research work has been carried out on the application of Neural Networks (NNs) to properly represent power system stability/security margins. For example, in [11], an NN approach to assess power sys-

tem stability based on training samples from off-line stability studies is presented. In [12], state-variable values are computed for a given set of contingencies, and these are then used as inputs to an NN to predict a transient stability margin. Similarly, making use of “nomograms”, the system security boundary is characterized by means of critical system parameters randomly generated to yield an NN input training set in [13]; the NN is then trained and tested obtaining a security boundary representation. A Back-Propagation Neural Network (BPNN) is used in [14] to predict voltage instabilities using as inputs both system load information and a voltage stability index; based on these inputs, the BPNN is used to predict new voltage stability index values for different operating scenarios. Also, making use of a trained BPNN, a representation of the system stability boundary is proposed in [15] to predict the available transfer capability of a system for any given dispatch. Finally, a novel approach based on BPNNs to obtain explicit differentiable functions of the system stability/security boundaries is presented in [16]. This methodology allows the introduction of the boundaries characterized by BPNNs as constraints in OPF models. The effectiveness and feasibility of the approach is demonstrated through the implementation and test of an OPF model for optimal dispatch and load curtailment in the context of competitive electricity markets.

The current paper uses the BPNN-based security boundary (SB) representation methodology presented in [16] to provide a more robust model of security limits within the typical DC-OPF models used in energy dispatch and market clearing auction mechanisms. A single-period and a multi-period Security-Boundary-Constrained DC-OPF (SBC DC-OPF) models for optimal dispatch are proposed, illustrated, tested and compared with respect to the classical Security-Constrained DC-OPF (SC DC-OPF) models using the well-known IEEE 2-area system. It should be mentioned that since the obtained BPNN-based SB is a nonlinear function of the OPF variables, the obtained SBC auction model is nonlinear; the proper linearization of the SBC-BPNN has presented some significant challenges and is currently under investigation.

The rest of the paper is structured as follows: Section 2 presents the classical SC DC-OPF-based models that form the basis of various existing auction systems; the typical representation of system security in these models, as well as the advantages and disadvantages of each model are also briefly discussed. Section 3 describes the proposed SBC OPF multi-period dispatch model, and presents the BPNN-based technique to estimate the security boundary function. Section 4 discusses the results obtained from the application of the proposed dispatch model to the two-area benchmark system, demonstrating its benefits. Finally, Section 5 summarizes and highlights the main results and contributions of this paper, and discusses future research directions.

2 SECURITY CONSTRAINED MARKET CLEARING AND DISPATCH MODELS

This section describes in some detail the basic DC-OPF models and concepts behind auction systems used in practice by system operators nowadays.

2.1 SC DC-OPF

A typical DC-OPF-based auction and dispatch model is basically a linear programming problem, consisting of optimizing a specific linear objective function, subject to a set of linear equality and inequality constraints. Since in most competitive electricity markets loads are for all practical purposes inelastic, the objective function is basically the minimization of the total cost function. In this case, the market clearing and dispatch mechanism assumes the following optimization problem formulation [17]:

$$\begin{aligned} \text{Min} \quad & \sum_{i=1}^n C_i P_{G_i} \\ \text{s.t.} \quad & P_{G_k} - P_{L_k} - \sum_{m=1, m \neq k}^N (P_{km}^{loss} + P_{km}) = 0 \quad \forall k \in \text{Bus} \\ & P_{km} - b_{km}(\delta_k - \delta_m) = 0 \quad \forall k, m, k \neq m \in \text{Bus} \\ & P_{km}^{min} \leq P_{km} \leq P_{km}^{max} \quad \forall k, m, k \neq m \in \text{Bus} \\ & P_{G_i}^{min} \leq P_{G_i} \leq P_{G_i}^{max} \quad \forall i \in \text{Gen} \end{aligned} \quad (1)$$

where C_i represents the cost coefficients or bids for the i^{th} generator in \$/MW; P_{G_i} is the real power generated by the i^{th} generator participating in the bidding, in MW, with minimum and maximum limits $P_{G_i}^{min}$ and $P_{G_i}^{max}$, respectively; P_{G_k} stands for the real power injected at bus k , which is basically P_{G_i} or zero if there is no generation at bus k ; P_{L_k} represents the load at bus k ; δ is the bus voltage phasor angle; b_{km} represents the transmission system admittance between buses k and m ; and P_{km} stands for the power flowing through the transmission element between buses k and m , which is used to represent system security by imposing limits on these power flows. The system losses P_{km}^{loss} can be modeled using a piece-wise linear (PWL) approximation of the losses in the transmission lines, as discussed in [18], as follows:

$$P_{km}^{loss} = g_{km} \sum_{l=1}^L \alpha_{km}(l) \delta_{km}(l) \quad (2)$$

where $\alpha_{km}(l)$ is the slope of the l^{th} segment of the linearized angle difference relative to the buses k and m , and g_{km} is the conductance of the line connecting these buses.

In model (1), P_{km} limits are usually obtained by means of off-line loadability and stability studies. Thus, these analyses are performed for a variety of dispatch and load scenarios, considering the “worst” system contingencies based on, at least, an $N - 1$ contingency criterion, i.e. accounting for the worst single contingencies in the system (in most systems, certain significant double contingencies are also considered). In this security analysis procedure, the maximum transfer condi-

tions may correspond to thermal limits in the transmission system equipment, bus voltage limits, voltage stability limits and/or angle stability limits. Since these limits are determined using operating conditions that do not necessarily represent actual solutions of the SC-DC-OPF-based auction, especially if the bidding is such that these solutions correspond to dispatch conditions not considered during the off-line security studies, this model may lead in some cases to insecure operating conditions and/or inappropriate price signals [1].

2.2 Multi-period SC DC-OPF

These types of auction and dispatch models are typically SC-DC-OPF problems representing several intervals in a given time window, so that inter-temporal constraints, such as ramp-up and ramp-down constraints in generators, can be properly modeled. Thus, based on (1) and considering the desired window of operation of the system, the multi-period SC-DC-OPF model takes the following form [17], [18], [19]:

$$\begin{aligned}
& \text{Min} \sum_{t=1}^T \sum_{i=1}^n C_i P_{G_i} \\
& \text{s.t. } P_{G_{k,t}} - P_{L_{k,t}} - \sum_{m=1, m \neq k}^N (P_{km,t}^{loss} + P_{km,t}) = 0 \quad \forall k \in \text{Bus}, \forall t \\
& P_{km,t} - b_{km} \cdot (\delta_{k,t} - \delta_{m,t}) = 0 \quad \forall k, m, k \neq m \in \text{Bus}, \forall t \\
& P_{km}^{min} \leq P_{km,t} \leq P_{km}^{max} \quad \forall k, m, k \neq m \in \text{Bus}, \forall t \\
& P_{G_i}^{min} \leq P_{G_i,t} \leq P_{G_i}^{max} \quad \forall i \in \text{Gen}, \forall t \\
& P_{G_i,t} - P_{G_i,t+1} \leq R_{DN_i} \quad \forall i \in \text{Gen}, \forall t \\
& P_{G_i,t+1} - P_{G_i,t} \leq R_{UP_i} \quad \forall i \in \text{Gen}, \forall t
\end{aligned} \quad (3)$$

where t stands for the time interval ($t = 1, \dots, T$), and R_{DN_i} and R_{UP_i} represent the ramp-down and ramp-up limits of the i^{th} generator, respectively. Once again, system security is represented through limits on the power flows in the transmission system computed off-line.

3 NEURAL NETWORK-BASED SECURITY BOUNDARY CONSTRAINED DC-OPF

An alternative approach to include security constraints into the DC-OPF formulation for electricity market is discussed in this section. Thus, an SB is first constructed by increasing the generators' outputs until the stability limits are reached for the worst contingencies ($N - 1$ contingency criteria plus important double contingencies), from a base operating point and for a variety of loading patterns, which in practice can be forecasted with significant accuracy due to the inelasticity of the demand. A BPNN is then used to approximate this boundary, and once it has been trained and tested, a closed form differentiable function that provides a mapping between the generator powers and the system's security status is generated. This function is finally used as a constraint in DC-OPF models similar to (1) and (3).

A full and detailed description of the SB BPNN model and computation methodology can be found in [16]. Hence, in this paper, only the most relevant principles and procedures associated with this technique are discussed.

3.1 Security Boundary Determination Procedure

The region where all the operating points can be reached without causing instability is called a "feasible region" [20]. At the boundary of this region, the system equilibrium points change their stability characteristics. The feasible region and the associated boundary can be constructed based on stability analyses of the differential-algebraic equations representing the power system [16]:

$$\begin{aligned}
\dot{x} &= h(x, y, u, p) \\
0 &= g(x, y, u, p)
\end{aligned} \quad (4)$$

where x is a vector of dynamic state variables; y is a vector of instantaneous state (algebraic) variables; u is a vector of "controllable" parameters associated with control settings; and p is a vector of "uncontrollable" parameters.

Since loads are inelastic and not really dispatchable, but are somewhat predictable with reasonable accuracy, whereas generators are dispatchable through an auction mechanism, feasibility boundaries are typically defined in practice with respect to generator power outputs (e.g. [21]). Hence, in this work, the SB, which is a stability boundary considering an $N - 1$ contingency criterion plus some relevant double contingencies, is assumed to be defined with respect to generator power outputs.

For each specific *dispatch direction* j (i.e. the rate of change of power of generators that have adequate reserve to serve a specific and forecastable load increase from the base load), the operating point may reach the system's feasibility boundary as the load increases, thus driving the system to unsecure or even unstable conditions. Let $K_{G_{ij}}$ be the factor of generated active power increase in a given generation direction defined by the "base" generation $P_{G_{ij_0}}$ for each generator i , for all participating generators, the generator output for a given loading point is then given by

$$P_{G_{ij}} = P_{G_{ij_0}} (1 + K_{G_{ij}}) \quad (5)$$

where $i = 1, 2, \dots, N_G$ (N_G is the number of participating generators) and $j = 1, 2, \dots, M$ (M is the number of directions considered).

For a generation direction j , the "critical" generators' power outputs are defined by the "critical" factors $K_{G_{ij}}^c$ needed to supply a given load increase until the SB is reached. The boundary can then be associated with these values and computationally approximated by means of a "critical generation matrix" as follows:

$$M_K = [c_1 \quad \dots \quad c_M] = \begin{bmatrix} K_{G_{11}}^c & \dots & K_{G_{1M}}^c \\ \vdots & \ddots & \vdots \\ K_{G_{N_G 1}}^c & \dots & K_{G_{N_G M}}^c \end{bmatrix} \quad (6)$$

This matrix, which is directly associated with the SB, is obtained by means of a combination of continuation power flow, eigenvalue and transient stability analyses

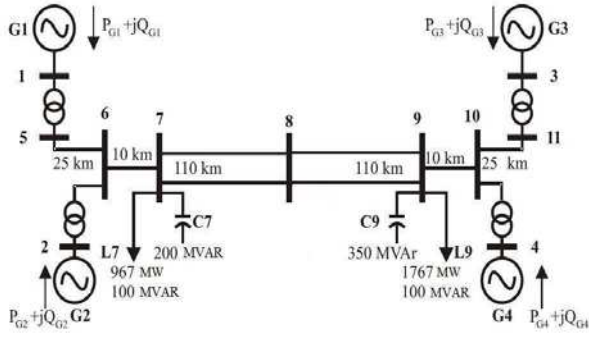


Figure 1: Two-area test system [22].

that allow to calculate the critical generator power factors $K_{G_{ij}}^c$ for the given loading conditions and relevant contingency criteria. The number of generation directions M is selected so that a reasonable density to correctly represent the SB is attained [16].

3.2 BPNN-based Security Boundary Mapping

The critical $K_{G_{ij}}^c$ values, which define the SB for the system model (4) along different generation directions for different loading conditions, can be used as training and testing sets of the BPNN to determine the SB mapping function. Thus, as explained in detail in [16], the SB can be approximated with the following nonlinear, closed-form, differentiable function:

$$K_{G_\ell}^c = \sum_{h=1}^H f_h \left[\left(\widehat{K}_G^T w^{in} + b_{in} \right) \cdot w_{21}^h + b_h \right] w_{32}^h + b_{out} = f(\widehat{K}_G) \quad (7)$$

where w , b and $f_h(\cdot)$ stand for the input (in), output (out) and hidden-layer neuron h weights, biases, and activation functions, respectively, of the BPNN; and $\widehat{K}_G^T = [K_{G_1} \dots K_{G_{\ell-1}} \ K_{G_{\ell+1}} \dots K_{G_{N_G}}]$ represents the $N_G - 1$ set of generation increases with respect to any given base value, i.e. $P_{G_i} = P_{G_{i_0}} (1 + K_{G_i})$ [16].

3.3 SBC OPF Models

The proposed SBC OPF dispatch model in its single-period formulation can then be formulated as follows:

$$\begin{aligned} \text{Min} \quad & \sum_{i=1}^{N_G} C_i P_{G_i} = \sum_{i=1}^{N_G} C_i P_{G_{i_0}} (1 + K_{G_i}) \\ \text{s.t.} \quad & P_{G_k} - P_{L_k} - \sum_{m=1, m \neq k}^N (P_{km}^{loss} + b_{km}(\delta_k - \delta_m)) = 0 \quad \forall k \in \text{Bus} \\ & K_{G_\ell}^c - f(\widehat{K}_G) \leq 0 \\ & P_{G_i}^{min} \leq P_{G_i} \leq P_{G_i}^{max} \quad \forall i \in \text{Gen} \end{aligned} \quad (8)$$

The penultimate equation in (8) above represents the SB constraint associated with the given loading conditions P_{L_k} . This constraint replaces the power flow limit constraints of model (1), and guarantees that the solution of the OPF problem remains within the required SB, as illustrated in the next section for a test system and various loading conditions.

Similarly, the multi-period dispatch model (3) can be transformed into the following SBC OPF model:

Gen	C [\$/MWh]	P_G^{max} [MW]	P_{G_0} [MW]	$R_{UP/DN}$ [MW/h]
G1	80	900	700	135
G2	80	900	700	135
G3	90	900	719	90
G4	90	900	700	90

Table 1: Generator data for the two-area system.

Loading	P_{L_7} [MW]	P_{L_9} [MW]
1	1389.63	1978.43
2	1452.74	2009.87

Table 2: Loading scenarios for two-area test system, single-period model.

Time Period	P_{L_7} [MW]	P_{L_9} [MW]
1	967	1767
2	1021.13	1983.53
3	1085	1982.6
4	1183	1983
5	1389.63	1978.43
6	1593.63	1923.66

Table 3: Loading scenarios for two-area test system, multi-period model.

$$\begin{aligned} \text{Min} \quad & \sum_{t=1}^T \sum_{i=1}^{N_G} C_{i,t} P_{G_{i,t}} = \sum_{t=1}^T \sum_{i=1}^{N_G} C_{i,t} P_{G_{i_0,t}} (1 + K_{G_{i,t}}) \\ \text{s.t.} \quad & P_{G_{k,t}} - P_{L_{k,t}} - \sum_{m=1, m \neq k}^N (P_{km,t}^{loss} + b_{km}(\delta_{k,t} - \delta_{m,t})) = 0 \quad \forall k \in \text{Bus}, \forall t \\ & K_{G_{\ell,t}}^c - f(\widehat{K}_{G_{\ell,t}}) \leq 0 \quad \forall t \\ & P_{G_i}^{min} \leq P_{G_{i,t}} \leq P_{G_i}^{max} \quad \forall i \in \text{Gen}, \forall t \\ & P_{G_{i,t}} - P_{G_{i,t+1}} \leq R_{DN_i} \quad \forall i \in \text{Gen}, \forall t \\ & P_{G_{i,t+1}} - P_{G_{i,t}} \leq R_{UP_i} \quad \forall i \in \text{Gen}, \forall t \end{aligned} \quad (9)$$

4 RESULTS

Numerical results of applying the SBC OPF proposed models to the IEEE 2-area system shown in Figure 1 are presented and discussed in this section. This system consists of two areas connected through a relatively weak double-circuit tie line. There are four generators at Buses 1, 2, 3 and 4, and two loads at Buses 7 and 9; the generators are grouped in two areas: G1 and G2 in Area A, and G3 and G4 in Area B; and the active power output of each generator is limited to 900 MW. All data for this system can be found in [22], and Table 1 shows the generator data required for the models and simulations.

Both the single-period (8) and the multi-period (9) models were applied, and the results were compared with respect to the corresponding “standard” SC DC-OPF models (1) and (3) to demonstrate the advantages of the proposed formulation with respect to basic market clearing and dispatch tools currently in use. The system SBs were obtained following the procedure discussed in Section 3.1, for 21 feasible and different generation directions for each generation area, based on static and dynamic studies (PSSs were included in all generators) and for the worst feasible single-contingency (Line 7-8 outage). A three-layered BPNN with 8 neurons in the hidden layer was trained to obtain the corresponding

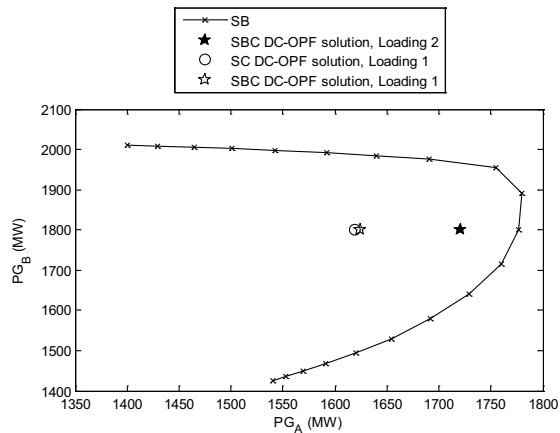


Figure 2: Security boundary and dispatch solutions for both single-period OPF models.

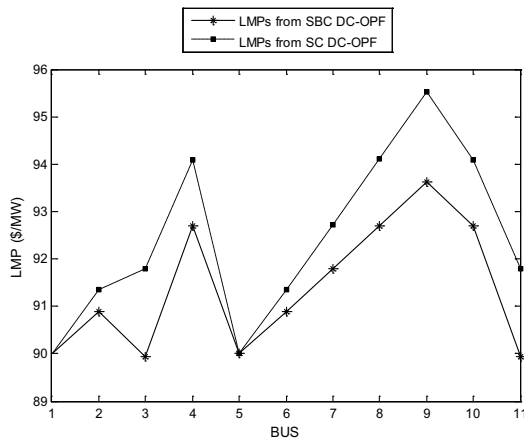


Figure 3: LMPs from single-period OPFs for Loading 1.

nonlinear mapping function (7), as explained in detail in [16].

In order to implement the single and multi-period simulations the various loading conditions shown in Tables 2 and 3 were considered. A different SB was obtained for each loading condition, as discussed in more detail next.

4.1 Single-period Simulations

The single-period models (1) and (8) were solved and compared for the two loading conditions shown in Table 2. The SB used in (8) for the two loading conditions assumed is depicted in Figure 2 in the area-generation parameter space. The security limits used in model (1) correspond to the transfer limits between the two areas, for one of the 21 generation directions used to obtain the SB.

The results obtained from solving the OPFs for the first loading scenario in Table 2 are illustrated in Tables 4 and 5, respectively, where $T = \sum_i P_{G_i}$ stands for the total power generated, i.e. the total “power transaction” levels. The area-generation powers obtained in this case are illustrated in Figure 2, and Figure 3 shows the corresponding LMPs at all buses. Observe from these tables and figures that basically both OPF models (1) and (8) yield, for all practical purpose, very similar results for Loading 1, with the SBC OPF generating slightly higher LMPs (about 10% higher). These similarity in the results is due to the fact that, as illustrated

Bus	Cost [\$]	LMP	P_G [MW]	P_L [MW]
1	651.58	90	723.98	0
2	810.00	90.89	900	0
3	720.00	89.94	900	0
4	720.00	92.69	900	0
5	0	90	0	0
6	0	90.89	0	0
7	0	91.79	0	1389.63
8	0	92.70	0	0
9	0	93.62	0	1978.43
10	0	92.69	0	0
11	0	89.94	0	0
TOTALS	Generation Cost= \$ 2,901.57		T=3,423.97 MW	Losses=55.68 MW

Table 4: Results for model (8), Loading 1.

Bus	Cost [\$]	LMP	P_G [MW]	P_L [MW]
1	647.08	90	718.98	0
2	810.00	91.35	900	0
3	720.00	91.80	900	0
4	720.00	94.09	900	0
5	0	90	0	0
6	0	91.35	0	0
7	0	92.72	0	1389.63
8	0	94.11	0	0
9	0	95.52	0	1978.43
10	0	94.09	0	0
11	0	91.80	0	0
TOTALS	Generation Cost= \$ 2,897.08		T=3,418.98 MW	Losses=47.84 MW

Table 5: Results for model (1), Loading 1

in Figure 2, the loading is such that the system is not close to its security limits.

When the load is increased to get closer to the SB, i.e. for Loading 2 in Table 2, both OPF models yield different results, with the SBC OPF (8) yielding the area-generation powers illustrated in Figure 2, whereas the SC DC-OPF (1) is infeasible in this case, i.e. no solutions were obtained. This can be justified in the less flexibility that characterizes the security modeling in (1) with respect to the SB representation. Observe in this figure that the system is much closer to its SB, as expected from the larger loading conditions.

4.2 Multi-period Simulations

The multi-period simulation corresponds to the solution of models (3) and (9) for the six time periods and associated loading conditions illustrated in Table 3.

The area-generation power and LMP results obtained from the simulations are shown in Figures 4 and 5. Note in Figure 4 that the dispatch levels obtained from both models are rather similar; however, model (3) yields an unsecure solution for the last time period. Also, as shown in Figure 5, the LMPs in most periods are about 10% higher for model (3) than the corresponding values obtained from the proposed model (9); this is due to the fact that, during most periods, the simplified representation of security limits in (3) over-constrain the system when compared to the proposed SB representation, as demonstrated above by the infeasibility of the SC DC-OPF model when the system conditions are close to the SB.

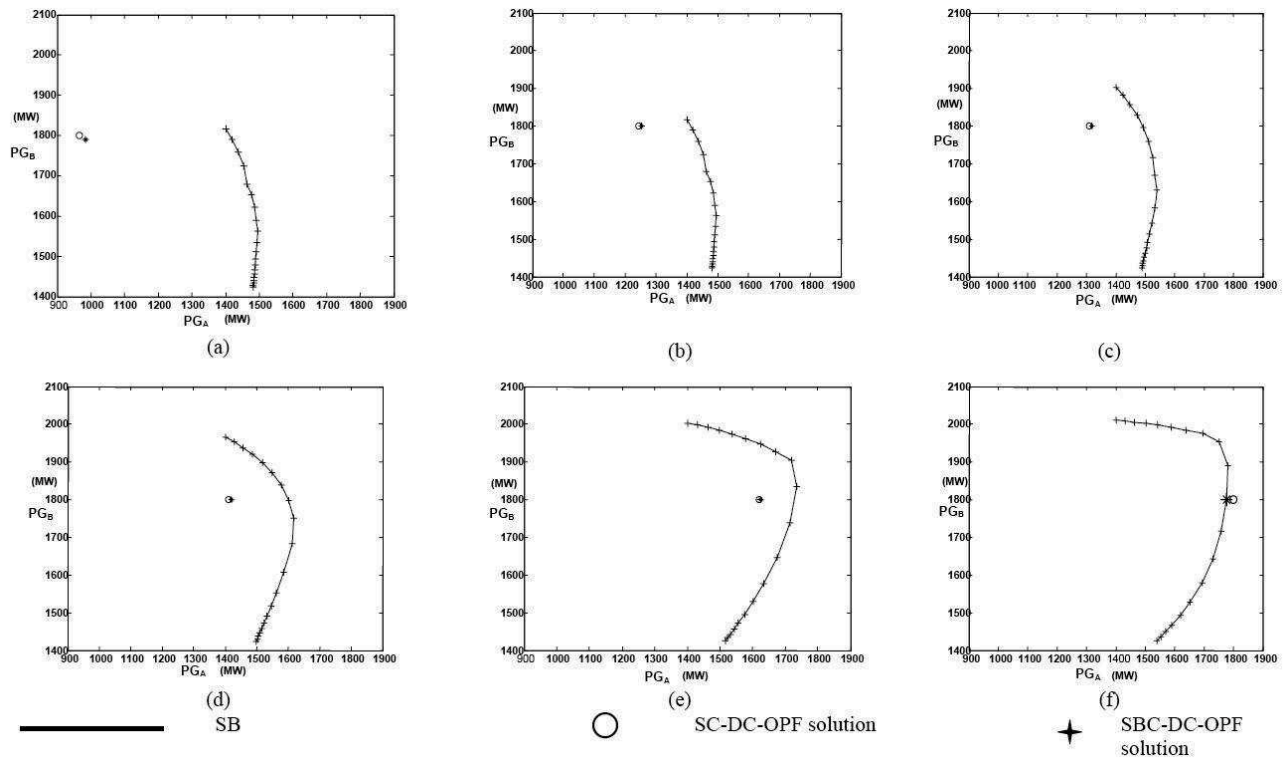


Figure 4: Area-generations obtained for both multi-period OPF models for the 6 time periods: (a) 1; (b) 2; (c) 3; (d) 4; (e) 5; and (f) 6.

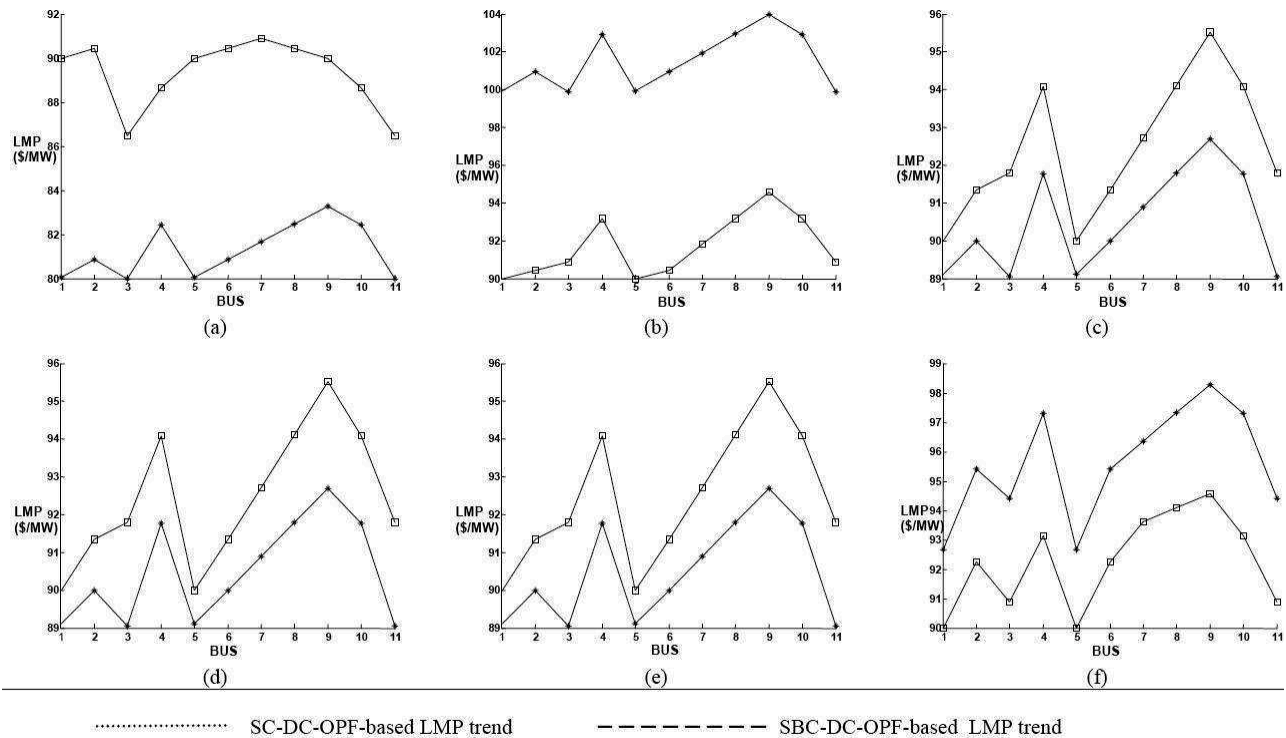


Figure 5: LMPs obtained for both multi-period OPF models for the 6 time periods: (a) 1; (b) 2; (c) 3; (d) 4; (e) 5; and (f) 6.

CONCLUSIONS

This paper proposed a new approach to model system security constraints in DC-OPF-based market clearing and dispatch mechanisms, based on the nonlinear representation obtained from a BPNN model of the security

boundary. This nonlinear function was directly used as a security constraint in a proposed SBC OPF model, in order to properly clear and dispatch a typical electricity market while ensuring that the optimal operating conditions are within a feasible and secure region. The proposed approach was tested using a benchmark system,

demonstrating its feasibility and advantages with respect to DC-OPF-based auction models currently used in practice.

The adequacy of the proposed SBC OPF model with respect to the widely-used SC DC-OPF model is demonstrated by the fact that, in general, it yields better pricing and system security conditions, at rather similar computational burden; moreover, the proposed model proved to be particularly effective for stressed system conditions. Therefore, the proposed auction algorithm should provide system operators with a more complete and reliable support tool for market clearing and power dispatch. However, given that the proposed SBC OPF model is nonlinear due to the presence of the NN SB function, whereas in practice most energy dispatch and market clearing mechanisms are based on linear DC-OPFs, the proper linearization of the proposed NN SB is currently being investigated.

REFERENCES

- [1] H. Ghasemi and A. Maria, "Benefits of Employing an On-line Security Limit Derivation Tool in Electricity Markets", in Proc. IEEE-PES General Meeting, July 2008.
- [2] "Final Report on the August 14, 2003 Blackout in the United States and Canada: Causes and Recommendations", US-Canada Power System Outage Task Force, April 2004.
- [3] C. A. Cañizares and S. K. M. Kotsi, "Power System Security in Market Clearing and Dispatch Mechanisms", in Proc. IEEE-PES General Meeting, June 2006, 6 pp.
- [4] D. Gan, R. J. Thomas, and R. D. Zimmerman, "Stability-Constrained Optimal Power Flow", IEEE Trans. Power Systems, vol. 15, no. 2, pp. 535-540, May 2000.
- [5] S. Bruno, E. D. Tuglie, and M. La Scala, "Transient Security Dispatch for the Concurrent Optimization of Plural Postulated Contingencies", IEEE Trans. Power Systems, vol. 17, no. 3, pp. 707-714, August 2002.
- [6] C. A. Cañizares, W. Rosehart, A. Berizzi, and C. Bovo, "Comparison of Voltage Security Constrained Optimal Power Flow Techniques", in Proc. IEEE-PES Summer Meeting, Vancouver, BC, Canada, pp. 1680-1685, July 2001.
- [7] S. K. M. Kotsi and C. A. Cañizares, "Application of a Stability Constrained Optimal Power Flow to Tuning of Oscillation Controls in Competitive Electricity Markets", IEEE Trans. Power Systems, vol. 22, no. 4, pp. 1944-1954, November 2007.
- [8] R. J. Avalos, C. A. Cañizares, and M. F. Anjos, "A Practical Voltage- Stability-Constrained Optimal Power Flow", in Proc. IEEE-PES General Meeting, July 2008.
- [9] B. Jayasekara and U. Annakkage, "Derivation of an Accurate Polynomial Representation of the Transient Stability Boundary", IEEE Trans. Power Systems, vol. 21, no. 4, pp. 1856-1863, November 2006.
- [10] J. A. Momoh, R. J. Koessler, M. S. Bond, B. Stott, D. Sun, A. Papalexopoulos, and P. Pistanovic, "Challenges to Optimal Power Flow", IEEE Trans. Power Systems, vol. 12, no. 1, pp. 444-455, February 1997.
- [11] M. Aggoune, M. A. El-Sharkawi, D. C. Park, M. J. Damborg, and R. J. Marks II, "Preliminary Results on Using Artificial Neural Networks for Security Assessment", IEEE Trans. Power Systems, vol. 6, no. 2, pp. 252-258, May 1991.
- [12] A. R. Eduards, K. W. Chan, R. W. Dunn, and A. R. Daniels, "Transient Stability Screening Using Artificial Neural Networks Within a Dynamic Security Assessment", IEE Proc. Generation, Transmission and Distribution, vol. 143, no. 2, pp. 129-134, March 1996.
- [13] J. D. McCalley, S. Wang, R. T. Treinen, and A. D. Papalexopoulos, "Security Boundary Visualization for Power Systems Operation", IEEE Trans. Power Systems, vol. 12, no. 2, pp. 940-947, May 1997.
- [14] S. Sahari, A. F. Abdin, and T. K. Rahaman, "Development of Artificial Neural Network for Voltage Stability Monitoring", in Proc. National Power Engineering Conference, pp. 37-42, December 2003.
- [15] X. Gu, and C. A. Cañizares, "Fast Prediction of Loadability Margins Using Neural Networks to Approximate Security Boundaries of Power Systems", IET Generation, Transmission and Distribution, vol. 1, no. 3, pp. 466-475, May 2007.
- [16] V. J. Gutierrez-Martinez, C. A. Cañizares, C. R. Fuente-Esquivel, A. Pizano-Martinez, and X. Gu, "Neural-Network Security-Boundary Constrained Optimal Power Flow", IEEE Trans. Power Systems, vol. 26, no. 1, pp. 63-72, February 2011.
- [17] G. B. Sheble, Computational Auction Mechanisms for Restructured Power Industry Operation, Kluwer Academic Publishers, Boston, 1998.
- [18] A. Motto, F. Galiana, A. Conejo, and J. Arroyo, "Network-constrained Multiperiod Auction for a Pool-Based Electricity Market", IEEE Trans. Power Systems, vol. 17, no. 3, pp. 646-653, August 2002.
- [19] C. N. Yu, A. I. Cohen, and B. Danai, "Multi-interval Optimization for Real-time Power System Scheduling in the Ontario Electricity Market", in Proc. IEEE-PES General Meeting, pp. 1296-1302, June 2005.
- [20] V. Venkatasubramanian, H. Schättler, and J. Zaborsky, "Local Bifurcations and Feasibility Regions in Differential-Algebraic Systems", IEEE Trans. on Automatic Control, vol. 40, no. 12, pp. 1992-2013, December 1995.
- [21] W. Li, Y. Mansour, E. Vaahedi, D.N. Pettet, "Incorporation of Voltage Stability Operating Limits in Composite System Adequacy Assessment: BC Hydro's Experience", IEEE Trans. Power Systems, vol. 13, no. 4, pp. 1279-1284, Nov. 1998.
- [22] P. Kundur, Power System Stability and Control, McGraw-Hill, 1994.

PRACTICAL SECURITY-BOUNDARY-CONSTRAINED DISPATCH MODELS FOR ELECTRICITY MARKETS

Response to Reviewers' Comments

1. *The first Paragraph of the abstract is not appropriate. Do you mean that other characterization of power system security are improper? Rather you could say that your approach to the subject is more robust.*

The Abstract and Introduction have been slightly revised to address this issue. This and other changes are highlighted in yellow.

2. *How do you choose the dispatch direction "j"? In Sec 4, you choose 21 directions. Is it necessary to choose 21 directions? Is it impossible to reduce the number of directions?*

A sentence to clarify this issue at the end of Section 3.1 has been added.

3. *If you choose so many directions, the calculation burden should be heavy. Did you compare the computation time between SC DC-OPF and your proposed SBC DC-OPF?*

The answer to this was provided in the Conclusions, where the computational burden for the SC DC OPF and SBC DC OPF is mentioned to be similar. Since the SB is determined off-line as discussed in section 3.1, this does not impact directly the computational burden of the proposed methodology.

4. *As the security boundary is calculated, when the operating point is not heavy, the results should require more margin to the boundary. Therefore, the result of SC DC-OPF is good. I think your proposed method is more effective to the severe condition. Is it right?*

Correct; thus, a sentence has been added to the Conclusions to make this clearer.

5. *In Sec 4.1, you mentioned SC DC-OPF is infeasible for Loading 2. Is it infeasible truly? Do you check the solution method of SC DC-OPF?*

The SC DC-OPF proved to be infeasible for Loading 2. A sentence to explain this outcome has been added to Sec. 4.1.

6. *In Sec 4.2, you point out that "the simplified representation of security limit in (3) over-constraint the system". I cannot agree it as I think it is opposite.*

We respectfully disagree with this statement, since the infeasibility of the SC DC-OPF when close to the SB clearly supports our statement. This argument has been added at the end of Section 4.2 to support this statement.

7. *In Figure 4, you insist that the solution of SC-DC-OPF violated the limits (might be under-constrained). On the other hand, in Figure 5, the limits in SC-DC-OPF were over-constrained. Why?*

We believe that this issue has been addressed in our response to comments 5 and 6.

8. *In Figure 5, the author said "LMPs for (3) is 10% higher than (9)". However, in (b) and (f), the LMP for SBC-OPF is higher than SC-OPF.*

Please note that the full statement reads “the LMPs *in most periods* are about 10% higher for model (3) than the corresponding values obtained from the proposed model (9)”, i.e. this refers to most and not all results.

9. *The axes on figure 4 and 5 are not clear.*

These figures’ axes have been clarified.

PRACTICAL SECURITY-BOUNDARY-CONSTRAINED DISPATCH MODELS FOR ELECTRICITY MARKETS

Claudia Battistelli¹, Claudio A. Cañizares², Mohammad Chehreghani Bozchalui²,
Victor J. Gutierrez-Martinez³, Claudio R. Fuerte-Esquivel³

¹ Federico II University, Naples, Italy

² University of Waterloo, Waterloo, Canada

³ Universidad Michoacana de San Nicolás de Hidalgo, Morelia, Mexico
ccanizar@uwaterloo.ca

Abstract – This paper concentrates **on a robust** characterization of system security, in terms of voltage collapse and oscillatory instabilities, in a “typical” multi-period DC-OPF auction and dispatch model. This characterization is based on the representation of the system security limits by means of a Neural Network (NN) approximation of the system security boundary. The proposed model is tested and compared with respect to a typical multi-period Security Constrained DC-OPF (SC-DC-OPF) model using the well-known two-area benchmark system. Results demonstrate that the approach ensures, in general, better locational marginal prices (LMPs) and guarantees that the operating points resulting from the optimization solution process are within the desired feasible and secure region, contrary to the typical multi-period SC-DC-OPF model, which may fail to meet this condition.

Keywords: *Optimal power flow, security constraints, neural networks, electricity markets, power dispatch, locational marginal pricing.*

1 INTRODUCTION

In the context of deregulated electricity markets, power systems operating close to their security limits have significant effect on prices and overall operating costs [1]. On the other hand, stability problems, particularly voltage collapse and oscillatory instabilities, have led to significant concerns on the part of system operators regarding the secure operation of power networks [2]. Therefore, the proper representation of system security in auction and dispatch models typically used by system operators for clearing and dispatching power markets has become quite relevant, since the typical accounting of system security by means of simple power transfer limits on transmission lines **could prove to be inadequate** [1]. The latter is due the fact that transmission limits do not always represent the actual security levels directly associated with the current market and system conditions, since they are determined off-line based on system operating conditions that do not necessarily correspond to the actual dispatch scenarios, which are mostly driven by market conditions at the time of dispatch, resulting in some cases in insecure operating conditions and/or inappropriate price signals [1], [3].

Several approaches to properly represent system security in OPF models, which are the base for market clearance and dispatch tools, have been proposed. For example, in [4], a stability-constrained OPF model is proposed based on a time-domain numerical representa-

tion of the dynamic equations which are included as constraints in the OPF process. In [5], a somewhat similar time-domain dispatch algorithm is proposed, but considering contingencies. In [6], the authors compare two different approaches to represent voltage security limits within OPF models; one is based on using the MSV of the power flow Jacobian, which is an index to detect proximity to voltage instability, as a security constraint, whereas the other is based on introducing the power flow equations associated with the voltage collapse point as additional constraints. An enhancement to the MSV approach is presented in [7], where oscillatory and voltage instability conditions are represented through a “dynamic” MSV stability index. The stability index used in [6] and [7] is an implicit function of the optimization variables, and hence their derivatives can be only approximated numerically in order to be included in the OPF solution process, leading to convergence problems and an approximation of the actual security limits. An improvement to this approach is presented in [8], where an MSV of an “equivalent” power flow Jacobian and an iterative procedure are proposed to explicitly represent the MSV security constraint in the OPF model. Finally, a differentiable function that can be readily introduced as a security constraint in an OPF model is proposed in [9]; in this case, the stability boundary is approximated by a polynomial obtained from an interpolation procedure and a nonlinear transformation applied to the system state variables.

All of proposed improvements available in the literature for the proper representation of security limits within dispatch and auction models are based on detailed and somewhat complex AC-OPF models. However, in practice, market clearing and dispatch mechanisms are based on DC-OPF multi-period models [3], given their significant computation advantages [10], such as less CPU-intensive computations and linear characteristics, which become more relevant in the multi-period models needed to represent ramp rates limits of generation units. Therefore, the current paper concentrates on the better representation of system security limits in a multi-period DC-OPF auction and dispatch model.

Extensive research work has been carried out on the application of Neural Networks (NNs) to properly represent power system stability/security margins. For example, in [11], an NN approach to assess power sys-

tem stability based on training samples from off-line stability studies is presented. In [12], state-variable values are computed for a given set of contingencies, and these are then used as inputs to an NN to predict a transient stability margin. Similarly, making use of “nomograms”, the system security boundary is characterized by means of critical system parameters randomly generated to yield an NN input training set in [13]; the NN is then trained and tested obtaining a security boundary representation. A Back-Propagation Neural Network (BPNN) is used in [14] to predict voltage instabilities using as inputs both system load information and a voltage stability index; based on these inputs, the BPNN is used to predict new voltage stability index values for different operating scenarios. Also, making use of a trained BPNN, a representation of the system stability boundary is proposed in [15] to predict the available transfer capability of a system for any given dispatch. Finally, a novel approach based on BPNNs to obtain explicit differentiable functions of the system stability/security boundaries is presented in [16]. This methodology allows the introduction of the boundaries characterized by BPNNs as constraints in OPF models. The effectiveness and feasibility of the approach is demonstrated through the implementation and test of an OPF model for optimal dispatch and load curtailment in the context of competitive electricity markets.

The current paper uses the BPNN-based security boundary (SB) representation methodology presented in [16] to provide a more robust model of security limits within the typical DC-OPF models used in energy dispatch and market clearing auction mechanisms. A single-period and a multi-period Security-Boundary-Constrained DC-OPF (SBC DC-OPF) models for optimal dispatch are proposed, illustrated, tested and compared with respect to the classical Security-Constrained DC-OPF (SC DC-OPF) models using the well-known IEEE 2-area system. It should be mentioned that since the obtained BPNN-based SB is a nonlinear function of the OPF variables, the obtained SBC auction model is nonlinear; the proper linearization of the SBC-BPNN has presented some significant challenges and is currently under investigation.

The rest of the paper is structured as follows: Section 2 presents the classical SC DC-OPF-based models that form the basis of various existing auction systems; the typical representation of system security in these models, as well as the advantages and disadvantages of each model are also briefly discussed. Section 3 describes the proposed SBC OPF multi-period dispatch model, and presents the BPNN-based technique to estimate the security boundary function. Section 4 discusses the results obtained from the application of the proposed dispatch model to the two-area benchmark system, demonstrating its benefits. Finally, Section 5 summarizes and highlights the main results and contributions of this paper, and discusses future research directions.

2 SECURITY CONSTRAINED MARKET CLEARING AND DISPATCH MODELS

This section describes in some detail the basic DC-OPF models and concepts behind auction systems used in practice by system operators nowadays.

2.1 SC DC-OPF

A typical DC-OPF-based auction and dispatch model is basically a linear programming problem, consisting of optimizing a specific linear objective function, subject to a set of linear equality and inequality constraints. Since in most competitive electricity markets loads are for all practical purposes inelastic, the objective function is basically the minimization of the total cost function. In this case, the market clearing and dispatch mechanism assumes the following optimization problem formulation [17]:

$$\begin{aligned} \text{Min} \quad & \sum_{i=1}^n C_i P_{G_i} \\ \text{s.t.} \quad & P_{G_k} - P_{L_k} - \sum_{m=1, m \neq k}^N (P_{km}^{loss} + P_{km}) = 0 \quad \forall k \in \text{Bus} \\ & P_{km} - b_{km}(\delta_k - \delta_m) = 0 \quad \forall k, m, k \neq m \in \text{Bus} \\ & P_{km}^{min} \leq P_{km} \leq P_{km}^{max} \quad \forall k, m, k \neq m \in \text{Bus} \\ & P_{G_i}^{min} \leq P_{G_i} \leq P_{G_i}^{max} \quad \forall i \in \text{Gen} \end{aligned} \quad (1)$$

where C_i represents the cost coefficients or bids for the i^{th} generator in \$/MW; P_{G_i} is the real power generated by the i^{th} generator participating in the bidding, in MW, with minimum and maximum limits $P_{G_i}^{min}$ and $P_{G_i}^{max}$, respectively; P_{G_k} stands for the real power injected at bus k , which is basically P_{G_i} or zero if there is no generation at bus k ; P_{L_k} represents the load at bus k ; δ is the bus voltage phasor angle; b_{km} represents the transmission system admittance between buses k and m ; and P_{km} stands for the power flowing through the transmission element between buses k and m , which is used to represent system security by imposing limits on these power flows. The system losses P_{km}^{loss} can be modeled using a piece-wise linear (PWL) approximation of the losses in the transmission lines, as discussed in [18], as follows:

$$P_{km}^{loss} = g_{km} \sum_{l=1}^L \alpha_{km}(l) \delta_{km}(l) \quad (2)$$

where $\alpha_{km}(l)$ is the slope of the l^{th} segment of the linearized angle difference relative to the buses k and m , and g_{km} is the conductance of the line connecting these buses.

In model (1), P_{km} limits are usually obtained by means of off-line loadability and stability studies. Thus, these analyses are performed for a variety of dispatch and load scenarios, considering the “worst” system contingencies based on, at least, an $N - 1$ contingency criterion, i.e. accounting for the worst single contingencies in the system (in most systems, certain significant double contingencies are also considered). In this security analysis procedure, the maximum transfer condi-

tions may correspond to thermal limits in the transmission system equipment, bus voltage limits, voltage stability limits and/or angle stability limits. Since these limits are determined using operating conditions that do not necessarily represent actual solutions of the SC-DC-OPF-based auction, especially if the bidding is such that these solutions correspond to dispatch conditions not considered during the off-line security studies, this model may lead in some cases to insecure operating conditions and/or inappropriate price signals [1].

2.2 Multi-period SC DC-OPF

These types of auction and dispatch models are typically SC-DC-OPF problems representing several intervals in a given time window, so that inter-temporal constraints, such as ramp-up and ramp-down constraints in generators, can be properly modeled. Thus, based on (1) and considering the desired window of operation of the system, the multi-period SC-DC-OPF model takes the following form [17], [18], [19]:

$$\begin{aligned}
& \text{Min} \sum_{t=1}^T \sum_{i=1}^n C_i P_{G_i} \\
& \text{s.t. } P_{G_{k,t}} - P_{L_{k,t}} - \sum_{m=1, m \neq k}^N (P_{km,t}^{loss} + P_{km,t}) = 0 \quad \forall k \in \text{Bus}, \forall t \\
& P_{km,t} - b_{km} \cdot (\delta_{k,t} - \delta_{m,t}) = 0 \quad \forall k, m, k \neq m \in \text{Bus}, \forall t \\
& P_{km}^{min} \leq P_{km,t} \leq P_{km}^{max} \quad \forall k, m, k \neq m \in \text{Bus}, \forall t \\
& P_{G_i}^{min} \leq P_{G_i,t} \leq P_{G_i}^{max} \quad \forall i \in \text{Gen}, \forall t \\
& P_{G_i,t} - P_{G_i,t+1} \leq R_{DN_i} \quad \forall i \in \text{Gen}, \forall t \\
& P_{G_i,t+1} - P_{G_i,t} \leq R_{UP_i} \quad \forall i \in \text{Gen}, \forall t
\end{aligned} \quad (3)$$

where t stands for the time interval ($t = 1, \dots, T$), and R_{DN_i} and R_{UP_i} represent the ramp-down and ramp-up limits of the i^{th} generator, respectively. Once again, system security is represented through limits on the power flows in the transmission system computed off-line.

3 NEURAL NETWORK-BASED SECURITY BOUNDARY CONSTRAINED DC-OPF

An alternative approach to include security constraints into the DC-OPF formulation for electricity market is discussed in this section. Thus, an SB is first constructed by increasing the generators' outputs until the stability limits are reached for the worst contingencies ($N - 1$ contingency criteria plus important double contingencies), from a base operating point and for a variety of loading patterns, which in practice can be forecasted with significant accuracy due to the inelasticity of the demand. A BPNN is then used to approximate this boundary, and once it has been trained and tested, a closed form differentiable function that provides a mapping between the generator powers and the system's security status is generated. This function is finally used as a constraint in DC-OPF models similar to (1) and (3).

A full and detailed description of the SB BPNN model and computation methodology can be found in [16]. Hence, in this paper, only the most relevant principles and procedures associated with this technique are discussed.

3.1 Security Boundary Determination Procedure

The region where all the operating points can be reached without causing instability is called a "feasible region" [20]. At the boundary of this region, the system equilibrium points change their stability characteristics. The feasible region and the associated boundary can be constructed based on stability analyses of the differential-algebraic equations representing the power system [16]:

$$\begin{aligned}
\dot{x} &= h(x, y, u, p) \\
0 &= g(x, y, u, p)
\end{aligned} \quad (4)$$

where x is a vector of dynamic state variables; y is a vector of instantaneous state (algebraic) variables; u is a vector of "controllable" parameters associated with control settings; and p is a vector of "uncontrollable" parameters.

Since loads are inelastic and not really dispatchable, but are somewhat predictable with reasonable accuracy, whereas generators are dispatchable through an auction mechanism, feasibility boundaries are typically defined in practice with respect to generator power outputs (e.g. [21]). Hence, in this work, the SB, which is a stability boundary considering an $N - 1$ contingency criterion plus some relevant double contingencies, is assumed to be defined with respect to generator power outputs.

For each specific *dispatch direction* j (i.e. the rate of change of power of generators that have adequate reserve to serve a specific and forecastable load increase from the base load), the operating point may reach the system's feasibility boundary as the load increases, thus driving the system to unsecure or even unstable conditions. Let $K_{G_{ij}}$ be the factor of generated active power increase in a given generation direction defined by the "base" generation $P_{G_{ij_0}}$ for each generator i , for all participating generators, the generator output for a given loading point is then given by

$$P_{G_{ij}} = P_{G_{ij_0}} (1 + K_{G_{ij}}) \quad (5)$$

where $i = 1, 2, \dots, N_G$ (N_G is the number of participating generators) and $j = 1, 2, \dots, M$ (M is the number of directions considered).

For a generation direction j , the "critical" generators' power outputs are defined by the "critical" factors $K_{G_{ij}}^c$ needed to supply a given load increase until the SB is reached. The boundary can then be associated with these values and computationally approximated by means of a "critical generation matrix" as follows:

$$M_K = [c_1 \quad \dots \quad c_M] = \begin{bmatrix} K_{G_{11}}^c & \dots & K_{G_{1M}}^c \\ \vdots & \ddots & \vdots \\ K_{G_{N_G 1}}^c & \dots & K_{G_{N_G M}}^c \end{bmatrix} \quad (6)$$

This matrix, which is directly associated with the SB, is obtained by means of a combination of continuation power flow, eigenvalue and transient stability analyses

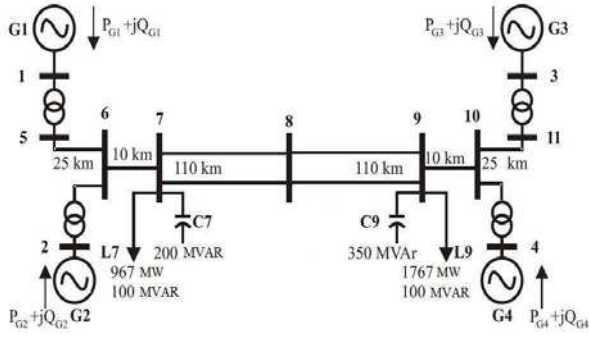


Figure 1: Two-area test system [22].

that allow to calculate the critical generator power factors $K_{G_{ij}}^c$ for the given loading conditions and relevant contingency criteria. The number of generation directions M is selected so that a reasonable density to correctly represent the SB is attained [16].

3.2 BPNN-based Security Boundary Mapping

The critical $K_{G_{ij}}^c$ values, which define the SB for the system model (4) along different generation directions for different loading conditions, can be used as training and testing sets of the BPNN to determine the SB mapping function. Thus, as explained in detail in [16], the SB can be approximated with the following nonlinear, closed-form, differentiable function:

$$K_{G_\ell}^c = \sum_{h=1}^H f_h \left[\left(\widehat{K}_G^T w^{in} + b_{in} \right) \cdot w_{21}^h + b_h \right] w_{32}^h + b_{out} = f(\widehat{K}_G) \quad (7)$$

where w , b and $f_h(\cdot)$ stand for the input (in), output (out) and hidden-layer neuron h weights, biases, and activation functions, respectively, of the BPNN; and $\widehat{K}_G^T = [K_{G_1} \dots K_{G_{\ell-1}} \ K_{G_{\ell+1}} \dots K_{G_{N_G}}]$ represents the $N_G - 1$ set of generation increases with respect to any given base value, i.e. $P_{G_i} = P_{G_{i_0}} (1 + K_{G_i})$ [16].

3.3 SBC OPF Models

The proposed SBC OPF dispatch model in its single-period formulation can then be formulated as follows:

$$\begin{aligned} \text{Min} \quad & \sum_{i=1}^{N_G} C_i P_{G_i} = \sum_{i=1}^{N_G} C_i P_{G_{i_0}} (1 + K_{G_i}) \\ \text{s.t.} \quad & P_{G_k} - P_{L_k} - \sum_{m=1, m \neq k}^N (P_{km}^{loss} + b_{km}(\delta_k - \delta_m) = 0 \quad \forall k \in \text{Bus} \\ & K_{G_\ell}^c - f(\widehat{K}_G) \leq 0 \\ & P_{G_i}^{min} \leq P_{G_i} \leq P_{G_i}^{max} \quad \forall i \in \text{Gen} \end{aligned} \quad (8)$$

The penultimate equation in (8) above represents the SB constraint associated with the given loading conditions P_{L_k} . This constraint replaces the power flow limit constraints of model (1), and guarantees that the solution of the OPF problem remains within the required SB, as illustrated in the next section for a test system and various loading conditions.

Similarly, the multi-period dispatch model (3) can be transformed into the following SBC OPF model:

Gen	C [\$/MWh]	P_G^{max} [MW]	P_{G_0} [MW]	$R_{UP/DN}$ [MW/h]
G1	80	900	700	135
G2	80	900	700	135
G3	90	900	719	90
G4	90	900	700	90

Table 1: Generator data for the two-area system.

Loading	P_{L_7} [MW]	P_{L_9} [MW]
1	1389.63	1978.43
2	1452.74	2009.87

Table 2: Loading scenarios for two-area test system, single-period model.

Time Period	P_{L_7} [MW]	P_{L_9} [MW]
1	967	1767
2	1021.13	1983.53
3	1085	1982.6
4	1183	1983
5	1389.63	1978.43
6	1593.63	1923.66

Table 3: Loading scenarios for two-area test system, multi-period model.

$$\begin{aligned} \text{Min} \quad & \sum_{t=1}^T \sum_{i=1}^{N_G} C_{i,t} P_{G_{i,t}} = \sum_{t=1}^T \sum_{i=1}^{N_G} C_{i,t} P_{G_{i_0,t}} (1 + K_{G_{i,t}}) \\ \text{s.t.} \quad & P_{G_{k,t}} - P_{L_{k,t}} - \sum_{m=1, m \neq k}^N (P_{km,t}^{loss} + b_{km}(\delta_{k,t} - \delta_{m,t}) = 0 \quad \forall k \in \text{Bus}, \forall t \\ & K_{G_{\ell,t}}^c - f(\widehat{K}_{G_{\ell,t}}) \leq 0 \quad \forall t \\ & P_{G_i}^{min} \leq P_{G_{i,t}} \leq P_{G_i}^{max} \quad \forall i \in \text{Gen}, \forall t \\ & P_{G_{i,t}} - P_{G_{i,t+1}} \leq R_{DN_i} \quad \forall i \in \text{Gen}, \forall t \\ & P_{G_{i,t+1}} - P_{G_{i,t}} \leq R_{UP_i} \quad \forall i \in \text{Gen}, \forall t \end{aligned} \quad (9)$$

4 RESULTS

Numerical results of applying the SBC OPF proposed models to the IEEE 2-area system shown in Figure 1 are presented and discussed in this section. This system consists of two areas connected through a relatively weak double-circuit tie line. There are four generators at Buses 1, 2, 3 and 4, and two loads at Buses 7 and 9; the generators are grouped in two areas: G1 and G2 in Area A, and G3 and G4 in Area B; and the active power output of each generator is limited to 900 MW. All data for this system can be found in [22], and Table 1 shows the generator data required for the models and simulations.

Both the single-period (8) and the multi-period (9) models were applied, and the results were compared with respect to the corresponding "standard" SC DC-OPF models (1) and (3) to demonstrate the advantages of the proposed formulation with respect to basic market clearing and dispatch tools currently in use. The system SBs were obtained following the procedure discussed in Section 3.1, for 21 feasible and different generation directions for each generation area, based on static and dynamic studies (PSSs were included in all generators) and for the worst feasible single-contingency (Line 7-8 outage). A three-layered BPNN with 8 neurons in the hidden layer was trained to obtain the corresponding

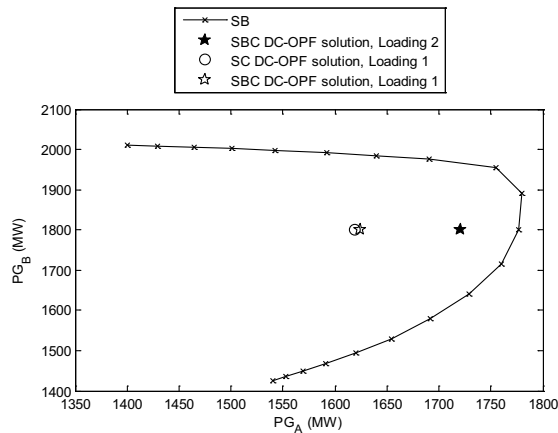


Figure 2: Security boundary and dispatch solutions for both single-period OPF models.

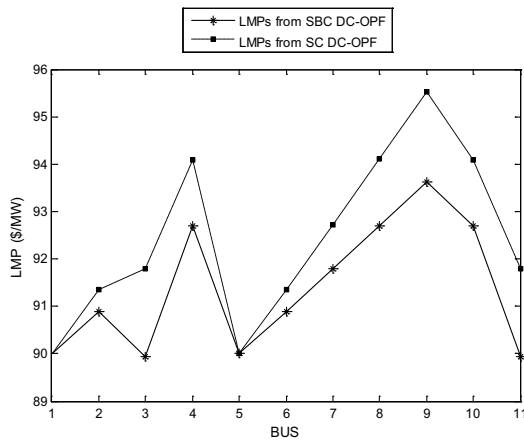


Figure 3: LMPs from single-period OPFs for Loading 1.

nonlinear mapping function (7), as explained in detail in [16].

In order to implement the single and multi-period simulations the various loading conditions shown in Tables 2 and 3 were considered. A different SB was obtained for each loading condition, as discussed in more detail next.

4.1 Single-period Simulations

The single-period models (1) and (8) were solved and compared for the two loading conditions shown in Table 2. The SB used in (8) for the two loading conditions assumed is depicted in Figure 2 in the area-generation parameter space. The security limits used in model (1) correspond to the transfer limits between the two areas, for one of the 21 generation directions used to obtain the SB.

The results obtained from solving the OPFs for the first loading scenario in Table 2 are illustrated in Tables 4 and 5, respectively, where $T = \sum_i P_{G_i}$ stands for the total power generated, i.e. the total “power transaction” levels. The area-generation powers obtained in this case are illustrated in Figure 2, and Figure 3 shows the corresponding LMPs at all buses. Observe from these tables and figures that basically both OPF models (1) and (8) yield, for all practical purpose, very similar results for Loading 1, with the SBC OPF generating slightly higher LMPs (about 10% higher). These similarity in the results is due to the fact that, as illustrated

Bus	Cost [\$]	LMP	P_G [MW]	P_L [MW]
1	651.58	90	723.98	0
2	810.00	90.89	900	0
3	720.00	89.94	900	0
4	720.00	92.69	900	0
5	0	90	0	0
6	0	90.89	0	0
7	0	91.79	0	1389.63
8	0	92.70	0	0
9	0	93.62	0	1978.43
10	0	92.69	0	0
11	0	89.94	0	0
TOTALS	Generation Cost= \$ 2,901.57		T=3,423.97 MW	Losses=55.68 MW

Table 4: Results for model (8), Loading 1.

Bus	Cost [\$]	LMP	P_G [MW]	P_L [MW]
1	647.08	90	718.98	0
2	810.00	91.35	900	0
3	720.00	91.80	900	0
4	720.00	94.09	900	0
5	0	90	0	0
6	0	91.35	0	0
7	0	92.72	0	1389.63
8	0	94.11	0	0
9	0	95.52	0	1978.43
10	0	94.09	0	0
11	0	91.80	0	0
TOTALS	Generation Cost= \$ 2,897.08		T=3,418.98 MW	Losses=47.84 MW

Table 5: Results for model (1), Loading 1

in Figure 2, the loading is such that the system is not close to its security limits.

When the load is increased to get closer to the SB, i.e. for Loading 2 in Table 2, both OPF models yield different results, with the SBC OPF (8) yielding the area-generation powers illustrated in Figure 2, whereas the SC DC-OPF (1) is infeasible in this case, i.e. no solutions were obtained. This can be justified in the less flexibility that characterizes the security modeling in (1) with respect to the SB representation. Observe in this figure that the system is much closer to its SB, as expected from the larger loading conditions.

4.2 Multi-period Simulations

The multi-period simulation corresponds to the solution of models (3) and (9) for the six time periods and associated loading conditions illustrated in Table 3.

The area-generation power and LMP results obtained from the simulations are shown in Figures 4 and 5. Note in Figure 4 that the dispatch levels obtained from both models are rather similar; however, model (3) yields an unsecure solution for the last time period. Also, as shown in Figure 5, the LMPs in most periods are about 10% higher for model (3) than the corresponding values obtained from the proposed model (9); this is due to the fact that, during most periods, the simplified representation of security limits in (3) over-constrain the system when compared to the proposed SB representation, as demonstrated above by the infeasibility of the SC DC-OPF model when the system conditions are close to the SB.

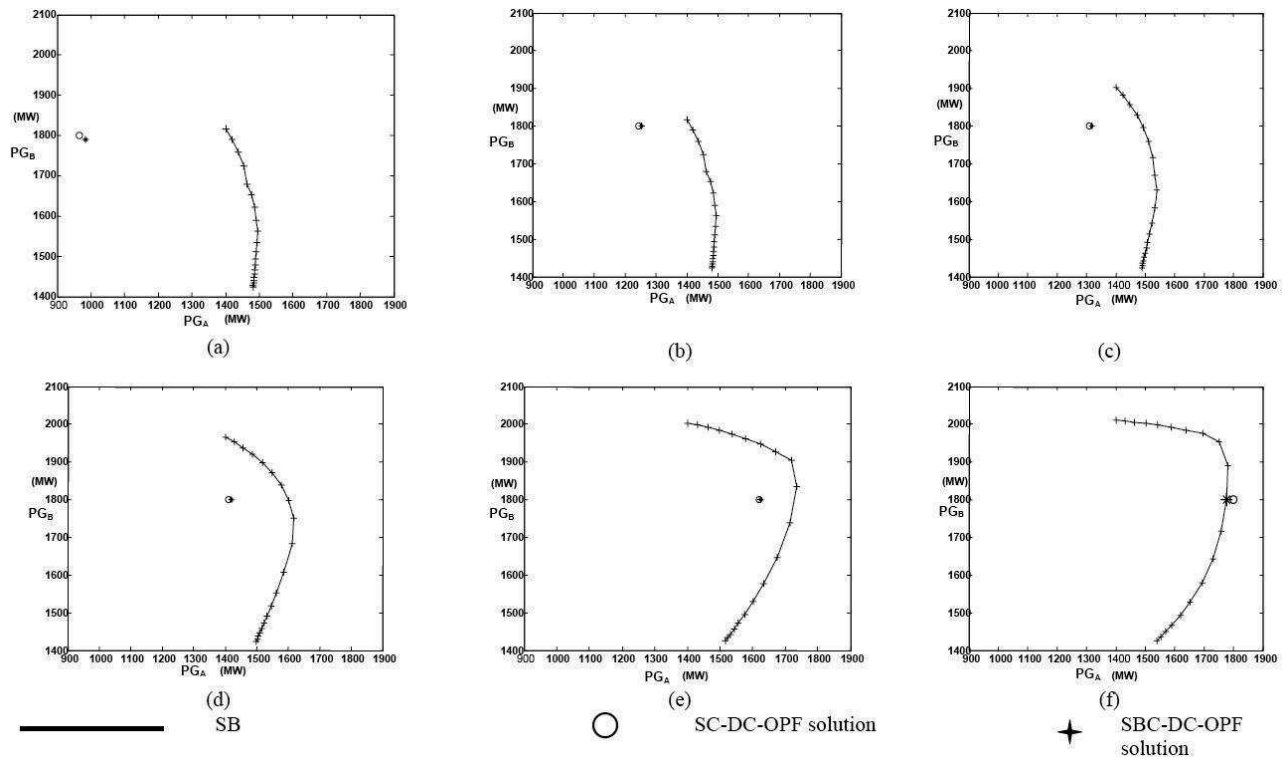


Figure 4: Area-generations obtained for both multi-period OPF models for the 6 time periods: (a) 1; (b) 2; (c) 3; (d) 4; (e) 5; and (f) 6.

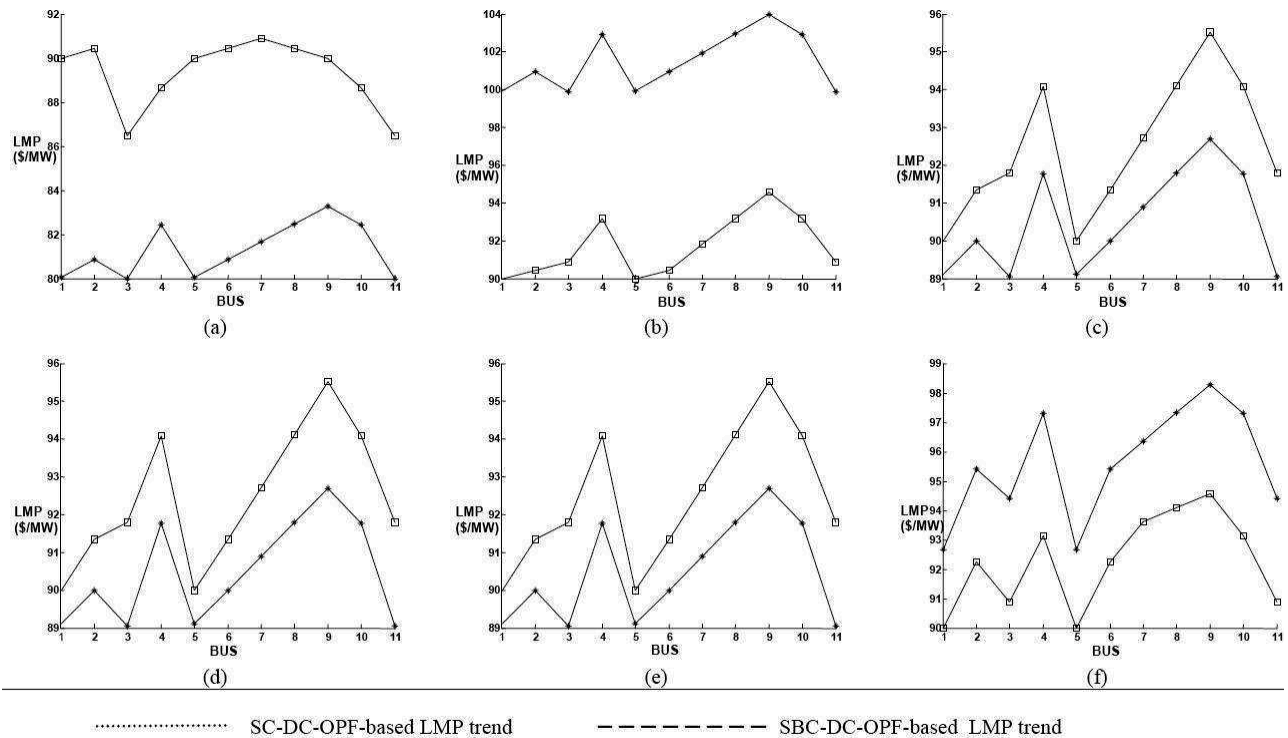


Figure 5: LMPs obtained for both multi-period OPF models for the 6 time periods: (a) 1; (b) 2; (c) 3; (d) 4; (e) 5; and (f) 6.

CONCLUSIONS

This paper proposed a new approach to model system security constraints in DC-OPF-based market clearing and dispatch mechanisms, based on the nonlinear representation obtained from a BPNN model of the security

boundary. This nonlinear function was directly used as a security constraint in a proposed SBC OPF model, in order to properly clear and dispatch a typical electricity market while ensuring that the optimal operating conditions are within a feasible and secure region. The proposed approach was tested using a benchmark system,

demonstrating its feasibility and advantages with respect to DC-OPF-based auction models currently used in practice.

The adequacy of the proposed SBC OPF model with respect to the widely-used SC DC-OPF model is demonstrated by the fact that, in general, it yields better pricing and system security conditions, at rather similar computational burden; moreover, the proposed model proved to be particularly effective for stressed system conditions. Therefore, the proposed auction algorithm should provide system operators with a more complete and reliable support tool for market clearing and power dispatch. However, given that the proposed SBC OPF model is nonlinear due to the presence of the NN SB function, whereas in practice most energy dispatch and market clearing mechanisms are based on linear DC-OPFs, the proper linearization of the proposed NN SB is currently being investigated.

REFERENCES

- [1] H. Ghasemi and A. Maria, "Benefits of Employing an On-line Security Limit Derivation Tool in Electricity Markets", in Proc. IEEE-PES General Meeting, July 2008.
- [2] "Final Report on the August 14, 2003 Blackout in the United States and Canada: Causes and Recommendations", US-Canada Power System Outage Task Force, April 2004.
- [3] C. A. Cañizares and S. K. M. Kotsi, "Power System Security in Market Clearing and Dispatch Mechanisms", in Proc. IEEE-PES General Meeting, June 2006, 6 pp.
- [4] D. Gan, R. J. Thomas, and R. D. Zimmerman, "Stability-Constrained Optimal Power Flow", IEEE Trans. Power Systems, vol. 15, no. 2, pp. 535-540, May 2000.
- [5] S. Bruno, E. D. Tuglie, and M. La Scala, "Transient Security Dispatch for the Concurrent Optimization of Plural Postulated Contingencies", IEEE Trans. Power Systems, vol. 17, no. 3, pp. 707-714, August 2002.
- [6] C. A. Cañizares, W. Rosehart, A. Berizzi, and C. Bovo, "Comparison of Voltage Security Constrained Optimal Power Flow Techniques", in Proc. IEEE-PES Summer Meeting, Vancouver, BC, Canada, pp. 1680-1685, July 2001.
- [7] S. K. M. Kotsi and C. A. Cañizares, "Application of a Stability Constrained Optimal Power Flow to Tuning of Oscillation Controls in Competitive Electricity Markets", IEEE Trans. Power Systems, vol. 22, no. 4, pp. 1944-1954, November 2007.
- [8] R. J. Avalos, C. A. Cañizares, and M. F. Anjos, "A Practical Voltage- Stability-Constrained Optimal Power Flow", in Proc. IEEE-PES General Meeting, July 2008.
- [9] B. Jayasekara and U. Annakkage, "Derivation of an Accurate Polynomial Representation of the Transient Stability Boundary", IEEE Trans. Power Systems, vol. 21, no. 4, pp. 1856-1863, November 2006.
- [10] J. A. Momoh, R. J. Koessler, M. S. Bond, B. Stott, D. Sun, A. Papalexopoulos, and P. Pistanovic, "Challenges to Optimal Power Flow", IEEE Trans. Power Systems, vol. 12, no. 1, pp. 444-455, February 1997.
- [11] M. Aggoune, M. A. El-Sharkawi, D. C. Park, M. J. Damborg, and R. J. Marks II, "Preliminary Results on Using Artificial Neural Networks for Security Assessment", IEEE Trans. Power Systems, vol. 6, no. 2, pp. 252-258, May 1991.
- [12] A. R. Eduards, K. W. Chan, R. W. Dunn, and A. R. Daniels, "Transient Stability Screening Using Artificial Neural Networks Within a Dynamic Security Assessment", IEE Proc. Generation, Transmission and Distribution, vol. 143, no. 2, pp. 129-134, March 1996.
- [13] J. D. McCalley, S. Wang, R. T. Treinen, and A. D. Papalexopoulos, "Security Boundary Visualization for Power Systems Operation", IEEE Trans. Power Systems, vol. 12, no. 2, pp. 940-947, May 1997.
- [14] S. Sahari, A. F. Abdin, and T. K. Rahaman, "Development of Artificial Neural Network for Voltage Stability Monitoring", in Proc. National Power Engineering Conference, pp. 37-42, December 2003.
- [15] X. Gu, and C. A. Cañizares, "Fast Prediction of Loadability Margins Using Neural Networks to Approximate Security Boundaries of Power Systems", IET Generation, Transmission and Distribution, vol. 1, no. 3, pp. 466-475, May 2007.
- [16] V. J. Gutierrez-Martinez, C. A. Cañizares, C. R. Fuente-Esquivel, A. Pizano-Martinez, and X. Gu, "Neural-Network Security-Boundary Constrained Optimal Power Flow", IEEE Trans. Power Systems, vol. 26, no. 1, pp. 63-72, February 2011.
- [17] G. B. Sheble, Computational Auction Mechanisms for Restructured Power Industry Operation, Kluwer Academic Publishers, Boston, 1998.
- [18] A. Motto, F. Galiana, A. Conejo, and J. Arroyo, "Network-constrained Multiperiod Auction for a Pool-Based Electricity Market", IEEE Trans. Power Systems, vol. 17, no. 3, pp. 646-653, August 2002.
- [19] C. N. Yu, A. I. Cohen, and B. Danai, "Multi-interval Optimization for Real-time Power System Scheduling in the Ontario Electricity Market", in Proc. IEEE-PES General Meeting, pp. 1296-1302, June 2005.
- [20] V. Venkatasubramanian, H. Schättler, and J. Zaborsky, "Local Bifurcations and Feasibility Regions in Differential-Algebraic Systems", IEEE Trans. on Automatic Control, vol. 40, no. 12, pp. 1992-2013, December 1995.
- [21] W. Li, Y. Mansour, E. Vaahedi, D.N. Pettet, "Incorporation of Voltage Stability Operating Limits in Composite System Adequacy Assessment: BC Hydro's Experience", IEEE Trans. Power Systems, vol. 13, no. 4, pp.1279-1284, Nov. 1998.
- [22] P. Kundur, Power System Stability and Control, McGraw-Hill, 1994.